RESEARCH ARTICLE | JULY 19 2023

How generic is iodide-tagging photoelectron spectroscopy: An extended investigation on the Gly·X^- (Gly = glycine, X = Cl or Br) complexes ⊘

Wenjin Cao ; Qinqin Yuan; Hanhui Zhang ; Xiaoguo Zhou ✉ ; Steven R. Kass ✉ ; Xue-Bin Wang ✉

Check for updates

View Online

Export Citation

CrossMark

How generic is iodide-tagging photoelectron spectroscopy: An extended investigation on the Gly·X^- (Gly = glycine, X = Cl or Br) complexes

Wenjin Cao,[1] iD   Qinqin Yuan,[1,2]   Hanhui Zhang,[1,3] iD   Xiaoguo Zhou,[3,a)] iD   Steven R. Kass,[4,a)] iD
and Xue-Bin Wang[1,a)] iD

AFFILIATIONS

[1] Physical Sciences Division, Pacific Northwest National Laboratory, Richland, Washington 99352, USA
[2] Key Laboratory of Structure and Functional Regulation of Hybrid Materials (Ministry of Education), Department
   of Chemistry, Anhui University, Hefei 230601, China
[3] Hefei National Laboratory for Physical Sciences at the Microscale, Department of Chemical Physics, University
   of Science and Technology of China, Hefei, Anhui 230026, People's Republic of China
[4] Department of Chemistry, University of Minnesota, Minneapolis, Minnesota 55455, USA

[a)] Authors to whom correspondence should be addressed: xzhou@ustc.edu.cn; kass@umn.edu; and xuebin.wang@pnnl.gov

ABSTRACT

We report a joint negative ion photoelectron spectroscopy (NIPES) and quantum chemical computational study on glycine-chloride/bromide complexes (denoted Gly·X^-, X = Cl/Br) in close comparison to the previously studied Gly·I^- cluster ion. Combining experimental NIPE spectra and theoretical calculations, various Gly·X^- complexes were found to adopt the same types of low-lying isomers, albeit with different relative energies. Despite more congested spectral profiles for Gly·Cl^- and Gly·Br^-, spectral assignments were accomplished with the guidance of the knowledge learned from Gly·I^-, where a larger spin–orbit splitting of iodine afforded well-resolved, recognizable spectral peaks. Three canonical plus one zwitterionic isomer for Gly·Cl^- and four canonical conformers for Gly·Br^- were experimentally identified and characterized in contrast to the five canonical ones observed for Gly·I^- under similar experimental conditions. Taken together, this study investigates both genericity and variations in binding patterns for the complexes composed of glycine and various halides, demonstrating that iodide-tagging is an effective spectroscopic means to unravel diverse ion-molecule binding motifs for cluster anions with congested spectral bands by substituting the respective ion with iodide.

Published under an exclusive license by AIP Publishing. https://doi.org/10.1063/5.0159326

I. INTRODUCTION

Amino acids (AAs) are ubiquitous in nature yet quite unique since they adopt canonical structures as isolated molecules while becoming charge separated in a zwitterionic form with the N-terminus protonated and the C-terminus deprotonated when solvated.[1,2] In addition to solvation, ion interactions, are also found to stabilize the zwitterionic form of AAs.[3–12] Moreover, binary AA-ion complexes serve as an important model system to understand ion-protein interactions, which play a crucial role in a wide range of physiological processes.[13–17] Therefore, numerous studies have been carried out to characterize AA-ion complexes, and the combina-

tion of infrared multiphoton dissociation (IRMPD) with theoretical calculations has been widely used in this regard.[3–12,18–20] Most of these reports have focused on cation-AA interactions whereas anion-AA complexes are much less studied.[21–25] In the former species, cations bind to the canonical form of the amino acid at electron rich sites or to the carboxylate group of a zwitterionic structure to form a salt bridge isomer. Anions, on the other hand, bind to electrophilic sites typically via hydrogen bond formation. A wide range of binding motifs are accessible in the anionic complexes due to the availability of multiple types of hydrogen bond donors (e.g., N–H, O–H, and C–H). This makes it difficult to characterize AA-anion structures due to their molecular complexity and the presence of

multiple conformers of varying energies. Furthermore, an efficient and sensitive spectroscopic tool is needed that can provide direct and recognizable signatures for an ensemble of conformers.

Recently, we proposed "iodide-tagging" negative ion photo-electron spectroscopy (NIPES) to probe multiple conformations of clusters with iodide ion binding to AAs ranging from the simplest one (i.e., glycine)[26] and its N-methylated derivatives[27] to arginine.[28] Through these studies, we observed not only the most stable conformers but also those within a certain energy window. We were also able to identify different binding patterns based on the vertical detachment energy (VDE) as the key spectral signature for distinguishing various conformers with different AA-iodide interaction energies. In the glycine-iodide complex, five low-lying isomers were clearly distinguishable as four well-resolved bands in the NIPE spectrum.[26] When replacing glycine with its N-methylated derivatives, conformational simplification was observed, mainly due to the replacement of strong hydrogen bond donors (N–H) with poorer ones (C–H).[27] This method was also applied to the arginine complex, which consisted of multiple canonical and zwitterionic isomers.[28] These studies showcased iodide-tagging NIPES as a sensitive probe for conformational identifications of iodide-containing complexes. One question that naturally arises from this work is: are the observed binding motifs specific to the iodide complexes, or do they represent a general binding pattern for a wide range of structurally similar anions with a given compound? The answer to this question will determine the utility of iodide-tagging NIPES and its generality for probing anion-molecular binding interactions. Consequently, the study of additional AA-anion complexes is of interest.

In this article, we present a combined NIPES and quantum chemical study on glycine-chloride and bromide clusters (denoted Gly·X^-, X = Cl and Br), focusing on the similarities and differences between the different halide anions. Since Cl^- and Br^- interact more strongly with neutral compounds than I^-, such a comparison provides an excellent platform to scrutinize their complex energy landscape as a function of ion-molecular interaction strength. We identified the same types of structures for Gly·Cl^- and Gly·Br^- as those located for Gly·I^-, albeit with larger energy gaps between the isomers, leading to fewer types of conformers being observed. The analogous binding patterns across the Cl–Br–I series suggest that the answer to the above question is that iodide tagging is a general approach and can be used as a model to probe distinct binding sites of complex molecules by taking advantage of their simplified spectral profiles to establish accurate conformational assignments. This, in turn, can provide a general way of addressing ion molecular systems with more complex spectral patterns.

II. METHODS

A. Negative ion photoelectron spectroscopy (NIPES)

NIPE spectra were obtained using a magnetic-bottle (MB) time-of-flight (TOF) photoelectron spectrometer combined with an electrospray ionization (ESI) source and a temperature-controlled cryogenic ion trap, as described elsewhere.[29] The anion complexes were generated by electrospraying ~0.1 mM mixtures of glycine and a halide salt (NaCl or KBr for Gly·Cl^- and Gly·Br^-, respectively) in a 1:1 ratio using acetonitrile/water (3:1 v/v) as the solvent. The resulting anions were transported by a radio frequency quadrupole ion guide and first detected with a quadrupole mass spectrometer in

order to optimize the ESI conditions to ensure stable and intense ion cluster beams. A 90° bender was used to direct the anions into the cryogenic 3D ion trap, where they were accumulated for 20–100 ms and cooled by collisions with a cold buffer gas (20% H_2 balanced in He) to 20 K before being pulsed-out into the extraction zone of the TOF mass spectrometer for mass analysis at a repetition rate of 10 Hz. The Gly·Cl/Br^- cluster anions were mass-selected and decelerated before being photodetached by a probe laser beam in the interaction zone of the MB photoelectron analyzer. A 193 nm (6.424 eV, Lambda Physics Complex 100 ArF) laser beam operated at a 20 Hz repetition rate was used for photodetachment, with the anion beam off on alternating laser shots to afford shot-to-shot background subtraction. The resulting photoelectrons were collected at nearly 100% efficiency and analyzed with a 5.2 m-long electron flight tube. Recorded flight times were converted into calibrated kinetic energies using the known spectrum of I^-/$Cu(CN)_2{}^-$.[30,31] Electron binding energies (EBEs) were obtained by subtracting the electron kinetic energies from the detachment photon energy with an electron energy resolution ($\Delta E/E$) of about 2% (i.e., ~20 meV for 1 eV kinetic energy electrons).

B. Computational details

Numerous initial structures for the Gly·Cl^- and Gly·Br^- cluster anions in zwitterionic and canonical forms were generated by Molclus[32] and pre-optimized using the semi-empirical quantum mechanical GFN2-xTB method.[33] Subsequent density functional theory (DFT) optimizations and frequency analyses were carried out without any symmetry constraints for selected low-lying isomers using the hybrid functional M06-2X[34] coupled with the def2-TZVP basis set[35] and Grimme's D3 dispersion corrections.[36] The selection of the M06-2X functional was based on extensive benchmarks on various amino acid-halide cluster anions.[27,28,37] The energy of each optimized anion and neutral radical at the anion geometry was refined by coupled-cluster single-point energy calculations with single-, double-, and perturbative triple-excitations [CCSD(T)][38,39] and the aug-cc-pVTZ[40,41] (aug-cc-pVTZ-PP for Br[42]) basis set. VDEs were calculated as the energy differences between the neutral and anionic clusters, both at the optimized anion geometries, whereas the relative energies of different anion isomers were calculated based on their electronic energies with zero-point energy (ZPE) corrections at the DFT level. All DFT and CCSD(T) calculations were carried out using the ORCA 5.0.3 and Gaussian 16 software packages.[43–45] In addition, Franck–Condon factors (FCFs) for spectral simulations were computed with the ezSpectrum program.[46]

III. RESULTS AND DISCUSSIONS

A. NIPE spectra of Gly·X^- clusters (X = Cl, Br, and I)

Figure 1 compares the 193 nm T = 20 K NIPE spectra of Gly·X^- (X = Cl, Br, and I[26]) clusters with the glycine molecule bound to various halide ions. Similar to many simple halide containing clusters previously studied,[47–50] the resulting spectra are expected to be similar to those of isolated halide ions but shifted to higher EBEs due to the interactions between the molecule and halides. For glycine with multiple potential binding sites, a previous case study on the Gly·I^- complex has shown that the resulting spectrum consists of multiple peaks at characteristic EBEs corresponding to different
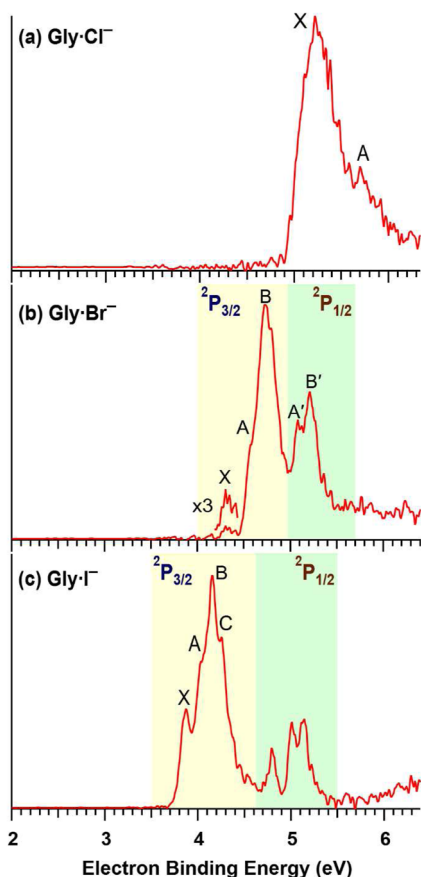
FIG. 1. T = 20 K NIPE spectra of Gly·X^- clusters (X = Cl, Br, and I) recorded at 193 nm. The Gly·I^- spectrum is adapted from Ref. 26.

isomers with different binding strengths [Fig. 1(c)].[26] At the incident photon energy of 193 nm (6.424 eV), two major band systems are resolved for Gly·Br^- and Gly·I^-, corresponding to the $^2P_{3/2}$ and $^2P_{1/2}$ spin–orbit states of the Br and I atoms (marked in yellow and green in Fig. 1), respectively. However, for the Gly·Cl^- complex, these two transitions merged into one broadband due to the small spin–orbit splitting of Cl (0.109 eV[51]) that prevents the two corresponding bands in the Gly·Cl^- complex from being resolved.

According to our previous investigation, the $^2P_{3/2}$ band in the Gly·I^- spectrum is further resolved into four peaks located at 3.85, 4.01, 4.15, and 4.26 eV, respectively (labeled as **X**, **A**, **B**, and **C**). In comparison, the Gly·Br^- spectrum [Fig. 1(b)] exhibits fewer resolved bands, with the most intense band **B** located at 4.74 eV (Table I), coupled with a shoulder on the lower EBE side at 4.58 eV labeled **A**. This feature is assigned as a distinct band since the corresponding peak within the $^2P_{1/2}$ band is clearly resolved from the more intense one at higher EBE [the corresponding peaks within the $^2P_{1/2}$ band are labeled **A′** and **B′** in Fig. 1(b)]. In addition, there is an extra weak band at 4.33 eV labeled **X**. For Gly·Cl^-, one broad band **X** centered at 5.22 eV is observed. It possesses a relatively sharp rising edge with some additional features on the higher EBE side, possibly attributed to transitions to the Cl $^2P_{1/2}$ spin–orbit states as well as

those coupled with certain vibrational modes. There is also a clearly visible shoulder **A** in the blue of this band at 5.71 eV, attributed to either vibrational coupling or a different isomer with a higher VDE. Although such a feature was observed for other chloride containing complexes,[48–50] its higher-than-normal relative intensity to the main band **X** indicates that there is a high probability that there is an additional isomer present with a larger VDE.

The binding energies of glycine—halide anion clusters can be estimated by comparing the VDEs of the complexes to those of the isolated halides. The shift in VDE (ΔVDE), defined as ΔVDE = VDE(Gly·X^-) − VDE(X^-) serves as a direct estimate of the dissociation energy (Table I), since the interactions in neutral radicals are substantially weaker than those in anionic complexes and could, thus, be neglected. The ΔVDEs of the Gly·Cl^- conformers are calculated to be between 1.61 and 2.10 eV based on the previously measured 3.61 eV electron affinity of the Cl atom.[52] This indicates that there is a strong interaction between Gly and Cl^- in all of the isomers. For Gly·Br^-, subtracting the electron affinity of the Br atom (3.36 eV)[53] affords ΔVDEs ranging from 0.97 to 1.38 eV based on the smallest (**X**) and largest (**B**) EBE bands. For Gly·I^-, smaller ΔVDEs of 0.79–1.20 eV were obtained (the VDE of I^- is 3.06 eV[30]). This provides a clear descending trend in the observed ΔVDEs that follows the electronegativities of the halogens.

B. Computed isomers of Gly·Cl^- and Gly·Br^- complexes

In the previous study, six canonical isomers and one zwitterion were located for the Gly·I^- complex.[26] These conformers differ in the preferred binding motif between glycine and I^-. In ascending order with respect to their relative energies, they are **I**, with I^- bridging the –NH₂ and –COOH groups; **II**, with the I^- interacting with both the –NH₂ and adjacent CH₂ groups; **III**, also with I^- binding to the N- and C-termini; **IV**, with I^- binding to the N-terminus; **V** and **VI**, both with I^- binding to the C-terminus; and **Z**, with glycine in its zwitterionic form and I^- interacting with the –NH₃⁺ group (Fig. 2 and Table I). Based on our M06-2X(D3)/def2-TZVP geometric optimizations, the Gly·Cl^- and Gly·Br^- analogs were found to adopt the same structures as those predicted for the Gly·I^- complex. That is, both the Cl^- and Br^- cluster ions form six canonical isomers **I–VI** and one zwitterionic structure **Z**, as described above.

The relative energies of the different isomers for Gly·Cl^- and Gly·Br^- are compared based on the CCSD(T)/aug-cc-pVTZ single point calculations, the same level of theory that was used in the previous study of Gly·I^- (Table I and Fig. 3). For Gly·Cl^-, **I** is also the most stable isomer, closely followed by **II** and **III** with energy differences of 0.88 and 1.63 kcal/mol, respectively. This trend is similar to that for Gly·I^- but with slightly larger energy gaps (Table I). Three additional canonical structures, **IV**, **V**, and **VI**, were located with higher relative energies of 5.09, 4.89, and 5.89 kcal/mol, respectively. These values for the latter three isomers of the Gly·Cl^- complex are also noticeably higher than those for Gly·I^-, especially for **IV**, where the Cl^- binds exclusively to the –NH₂. Zwitterionic isomer **Z** is less stable than **I–V** and similar to **VI** with a relative energy of 5.66 kcal/mol. This makes it noticeably more stable than the analogous Gly·I^- complex, which has a relative energy of 7.49 kcal/mol.

Substitution of I^- with Br^- also leads to six canonical structures with relative energies spanning 6.11 kcal/mol. The most stable

TABLE I. Calculated CCSD(T) relative energies (E, in kcal/mol) and VDEs (in eV) of the different Gly·X^- (X = Cl, Br, and I) isomers along with the experimental band positions (Expt., in eV). Parenthetical values and letters are the ΔVDEs and band assignments in accordance with the labeling in Fig. 1.
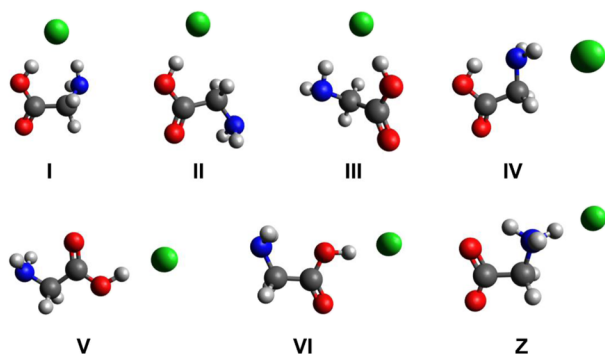
	Gly·Cl^-			Gly·Br^-			Gly·I^{-} [a]		
	E	VDE	Expt.[b]	E	VDE	Expt.[b]	E	VDE	Expt.[b]
I	0	5.22	5.22 (1.61, **X**)	0	4.79	4.74 (1.38, **B**)	0	4.30	4.26 (1.20, **C**)
II	0.88	5.08	5.22 (1.61, **X**)	0.99	4.62	4.58 (1.22, **A**)	0.45	4.16	4.15 (1.09, **B**)
III	1.63	5.20	5.22 (1.61, **X**)	1.50	4.78	4.74 (1.38, **B**)	1.34	4.30	4.26 (1.20, **C**)
IV	5.09	4.63	⋯	3.91	4.31	4.33 (0.97, **X**)	1.57	3.96	4.01 (0.95, **A**)
V	4.89	4.83	⋯	5.13	4.29	⋯	3.93	3.83	3.85 (0.79, **X**)
VI	5.89	4.89	⋯	6.11	4.34	⋯	5.10	3.86	⋯
Z	5.66	5.68	5.71 (2.10, **A**)	5.78	5.17	⋯	7.49	4.86	⋯

[a] From Ref. 26.
[b] Experimental VDEs for Cl^-, Br^-, and I^- are 3.61, 3.36, and 3.06 eV (see Refs. 30, 52, and 53, respectively).
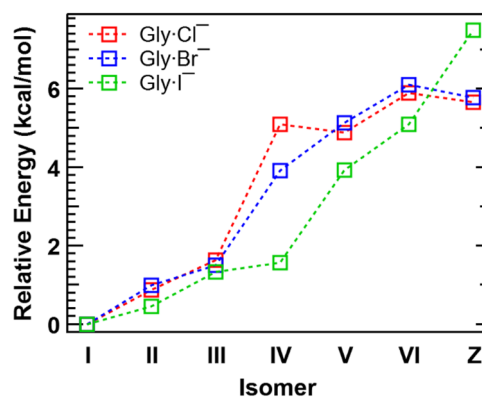
isomers (**I**, **II**, and **III**) have relative energies of 0, 0.99, and 1.50 kcal/mol and similar energy gaps compared to those for Gly·Cl^-. A sharp decrease in stability is also observed for **IV** relative to the analogous iodide complex (3.91 vs 1.57 kcal/mol), but the falloff is less than that for Gly·Cl^-. In both **V** and **VI**, the bromide anion binds just to the carboxyl group, and these two isomers are even higher in energy (i.e., 5.13 and 6.11 kcal/mol, respectively). Finally, the zwitterionic structure **Z** (5.78 kcal/mol) is more stable than **VI** and the analogous isomer for Gly·I^- but slightly less stable than the Gly·Cl^- zwitterion. These predictions are in accordance with the observation that the glycine-halide binding interactions grow stronger when going from I^- to Br^- and then Cl^-. This leads to stronger conformational preferences and less unfavorable zwitterionic structures when X = Cl and Br. Not all of these isomers, however, are kinetically trapped and detected. For Gly·I^-, only **I** through **V** with relative energies up to 3.93 kcal/mol were observed. Due to the larger energy gaps for Gly·Cl^- and Gly·Br^-, fewer isomeric structures are apparent in the observed spectra.

C. Kinetically trapped isomers of Gly·Cl^- and Gly·Br^- complexes

To assign the experimental NIPE spectra, the VDEs of each isomer were computed at the CCSD(T)/aug-cc-pVTZ level of theory.

This method is not only the gold standard for computational chemistry but was also used to assign all of the key spectral features (**X**, **A**, **B**, and **C**) for Gly·I^- isomers **V**, **IV**, **II**, and **I/III**, respectively, based upon the excellent agreement between the experimental and calculated VDEs (Table I).[26] Moreover, FCF simulations were also carried out to examine the effects of vibrational couplings (Fig. S1). For the Gly·Cl^- complex, the most stable isomer **I** possesses a calculated VDE of 5.22 eV, matching nicely with the experimental band maximum of 5.22 eV [Fig. 4(a)]. In addition, isomer **III**, with a relative energy of 1.63 kcal/mol and a similar binding motif, possesses a nearly identical calculated VDE of 5.20 eV and may also be present. Isomer **II** with a relative energy of 0.88 kcal/mol has a slightly smaller calculated VDE of 5.08 eV, but this is within the EBE range that the broad Gly·Cl^- spectrum spans [Fig. 4(a)]. Considering its relative stability, this isomer may be present and contribute to the rising edge of the most intense band leading to the broad spectrum. These three isomers are also present in the Gly·I^- cluster along with higher-energy isomers **IV** and **V** with relative energies of up to 3.93 kcal/mol.[26] For the Gly·Cl^- complex, **IV**, **V**, and **VI** have even higher relative energies but substantially lower calculated VDEs of 4.63, 4.83, and 4.89 eV, respectively. This indicates that these

FIG. 2. Optimized geometries of the six canonical (**I–VI**) and one zwitterionic (**Z**) forms of Gly·X^- (X = Cl, Br, and I). The C, N, O, H, and X atoms are represented with gray, blue, red, light gray, and green balls, respectively.

FIG. 3. Calculated CCSD(T)/aug-cc-pVTZ(-PP) relative energies of the various structures of the Gly·X^- clusters (X = Cl, Br, and I).
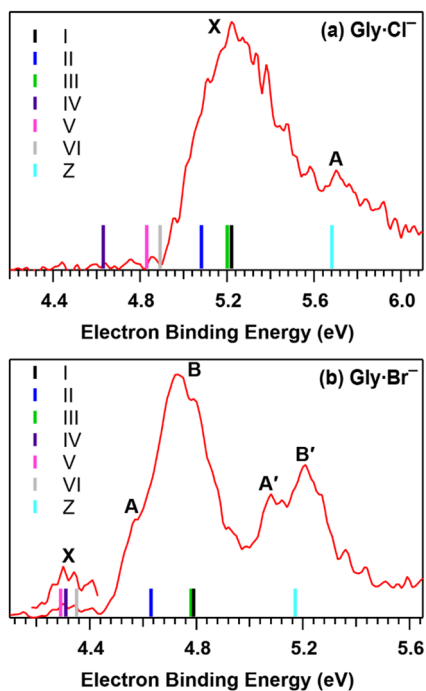
FIG. 4. CCSD(T)/aug-cc-pVTZ calculated VDEs of the different isomers of Gly·Cl⁻ (a) and Gly·Br⁻ (b) in comparison to their respective experimental spectra.
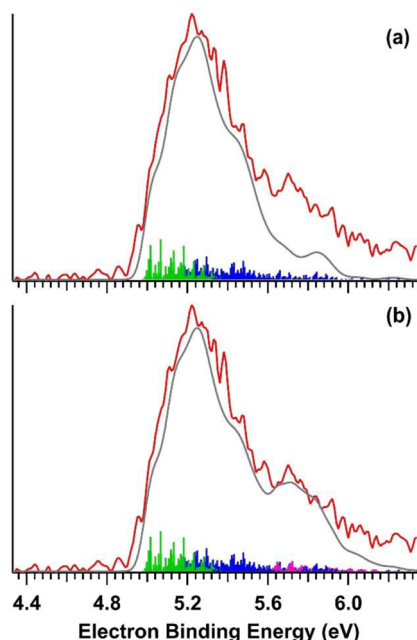

FIG. 5. Comparisons of FCF simulated spectra (gray trace) without (a) and with (b) the inclusion of zwitterionic isomer **Z** to the experimental NIPE spectrum (red trace) of the Gly·Cl⁻ complex. The FCF simulated sticks for isomers **I**, **II**, and **Z** are in blue, green, and pink, respectively, each containing two sets of transitions separated by ~0.1 eV, corresponding to the spin–orbit splitting in the Cl atom.

species do not contribute to the experimental NIPE spectrum since their calculated VDEs are at least 0.3 eV lower than the observed band maximum and are outside of the spectral bandwidth. Interestingly, the zwitterionic isomer **Z** also has a high relative energy (5.66 kcal/mol), but its computed VDE of 5.68 eV matches up well with band **A**. Given that zwitterionic structures of amino acids are known to be favored over their canonical forms in aqueous solution[1,2] and that electrospray ionization can afford liquid-phase isomers in preference to more stable gas-phase structures,[54–56] one cannot exclude **Z** from consideration simply due to its high energy. To determine whether it contributes to band **A**, FCF simulations were conducted with and without the inclusion of isomer **Z** for comparison to the experimental spectrum (Fig. 5). Isomers **I** and **III** have nearly identical computed VDEs (Table I) and similar FCF profiles (Fig. S1), so the spectral simulations only stack the FCF spectra of **I** and **II** with and without the inclusion of **Z**. Both instances consist of two datasets separated by ~0.1 eV to reproduce the spin–orbit coupling splitting. Despite certain spectral features at ~5.7 eV due to vibrational coupling in the simulated spectrum, the experimental band **A** is still clearly underestimated without the inclusion of isomer **Z** [Fig. 5(a)]. When it is taken into consideration, an excellent match with the experimental spectra is obtained [Fig. 5(b)]. Therefore, isomer **Z** contributes to the observed NIPE spectrum and is kinetically trapped during the experiment. This contrasts with the spectrum for Gly·I⁻, where the zwitterionic isomer was not observed. The reason for this difference may be due to the less unfavorable energetics for **Z** in Gly·Cl⁻ compared to Gly·I⁻, which could also result in a higher barrier between the zwitterionic and canonical forms in the former

complex [the barrier from **Z** to **IV** is 5.7 kJ/mol at the CCSDT/aug-cc-pVTZ//M06-2X(D3)/aug-cc-pVDZ level, while it is 8.2 kJ/mol at M06-2X(D3)/aug-cc-pVDZ]. The stronger interaction with the chloride anion also leads to larger energy gaps between the different canonical structures, resulting in fewer detected isomers in the Gly·Cl⁻ complex and the absence of **V** and **VI**, where Cl⁻ interacts only with the C-terminus.

For the Gly·Br⁻ complex, the three most stable isomers **I**, **II**, and **III** are clearly observed. The most intense band **B** is assigned to **I** and **III**, both of which have Br⁻ bridging between the –NH₂ and –COOH groups. The calculated VDEs for these two isomers are 4.79 and 4.78 eV, respectively, which are in excellent accordance with the experimental band position of 4.74 eV. Isomer **II** has the Br⁻ binding to the –NH₂ and CH₂ groups and a calculated VDE of 4.62 eV, which accounts for band **A** located at 4.58 eV. The other three canonical isomers **IV**, **V**, and **VI** have nearly identical calculated VDEs of 4.31, 4.29, and 4.34 eV, respectively, all of which seem to match the EBE of band **X** at 4.33 eV. Among them, **IV** is the most stable with a relative energy of 3.91 kcal/mol and is the most likely contributor to this band since an isomer with a relative energy of 3.93 kcal/mol for the Gly·I⁻ complex was also formed under identical experimental conditions.[26] Canonical isomers **V** and **VI** have higher energies (5.13 and 6.11 kcal/mol) and are less likely to be formed given that no Gly·Cl⁻ or Gly·I⁻ canonical structures with similar energies are observed. The relative intensity ratio of band **X** to the most intense band in the Gly·Br⁻ spectrum is substantially smaller compared to that for Gly·I⁻ (Fig. 1), despite both features being attributed to isomers with

similar relative energies (i.e., **IV** at 3.91 kcal/mol for Gly·Br⁻ vs **V** at 3.93 kcal/mol for Gly·I⁻). This difference suggests that two different types of isomers are responsible for **X**, which is in agreement with our assignments. In the case of isomer **V** of Gly·I⁻, the I⁻ is bound just to the C-terminus and has a short FC profile,[26] whereas isomer **IV** of Gly·Br⁻ has the Br⁻ bound to the N-terminus and a much broader spanning FCF simulated spectrum (Fig. S1). This is due to a larger structural change upon photodetachment, resulting in a much lower spectral intensity. Finally, zwitterionic isomer **Z** is also relatively unstable (5.78 kcal/mol) and has a high predicted VDE of 5.17 eV that falls into an EBE range that overlaps with the spin–orbit excited bands (bands **A′** and **B′**). Since the FCF simulation without **Z** nicely reproduces the experimental NIPE spectrum (Fig. S3), it is unlikely to be present under the employed experimental conditions.

IV. CONCLUSIONS

Employing NIPES and quantum chemical computations, the geometric structures of various isomers with a glycine molecule bound to either Cl⁻ or Br⁻ have been characterized. By comparing these results with a previous study on Gly·I⁻, the binding patterns in all three complexes are found to be similar. Six canonical and one zwitterionic isomers in nearly identical geometries were computationally located. The energy gaps are dependent upon the anion, leading to different numbers of kinetically trapped isomers under the same experimental conditions, i.e., three canonical and one zwitterionic isomers for Gly·Cl⁻, four canonical isomers for Gly·Br⁻, and five canonical isomer for the Gly·I⁻ complex. The zwitterionic isomer is exclusively observed for the Gly·Cl⁻ complex, consistent with its less unfavorable relative energy and greater anion binding energy, which may lead to a more appreciable zwitterionic—canonical transition barrier, enabling the dominant zwitterionic isomer in aqueous solution to be observed in the gas phase. These variations arise from the differences in binding strengths between glycine and the various anions. Nevertheless, all three cluster anions qualitatively follow the same general binding patterns and structural motifs. These similarities with different halides demonstrate the generality of the iodide-tagging approach and make it an attractive strategy for modeling the active binding sites of complexes of interest. The simplified spectral pattern of an iodide cluster ion makes it a useful system for analyzing distinct binding motifs, which in turn can provide crucial guidance toward analyzing ion molecular systems with more complex spectral patterns.

SUPPLEMENTARY MATERIAL

See the supplementary material for FCF simulations for each of the complexes (Figs. S1 and S2), a comparison of experimental and simulated spectra for the Gly·Br⁻ (Fig. S3), and cartesian coordinates and CCSD(T) energies of all computed cluster anions.

ACKNOWLEDGMENTS

AUTHOR DECLARATIONS

Conflict of Interest

The authors have no conflicts to disclose.

Author Contributions

Wenjin Cao: Data curation (equal); Formal analysis (lead); Investigation (lead); Writing – original draft (lead). **Qinqin Yuan**: Data curation (equal); Investigation (supporting). **Hanhui Zhang**: Data curation (supporting); Investigation (supporting). **Xiaoguo Zhou**: Conceptualization (equal); Funding acquisition (equal); Investigation (equal); Writing – review & editing (equal). **Steven R. Kass**: Conceptualization (equal); Formal analysis (equal); Funding acquisition (supporting); Investigation (equal); Writing – review & editing (equal). **Xue-Bin Wang**: Conceptualization (equal); Funding acquisition (equal); Project administration (equal); Writing – review & editing (equal).

DATA AVAILABILITY

The data that support the findings of this study are available within the article and its supplementary material.

REFERENCES

[1] M. J. Locke and R. T. McIver, "Effect of solvation on the acid/base properties of glycine," J. Am. Chem. Soc. **105**, 4226–4232 (1983).

[2] S. Xu, J. M. Nilles, and K. H. Bowen, Jr., "Zwitterion formation in hydrated amino acid, dipole bound anions: How many water molecules are required?," J. Chem. Phys. **119**, 10696–10701 (2003).

[3] M. F. Bush, J. T. O'Brien, J. S. Prell, R. J. Saykally, and E. R. Williams, "Infrared spectroscopy of cationized arginine in the gas phase: Direct evidence for the transition from nonzwitterionic to zwitterionic structure," J. Am. Chem. Soc. **129**, 1612–1622 (2007).

[4] M. F. Bush, J. Oomens, R. J. Saykally, and E. R. Williams, "Effects of alkaline earth metal ion complexation on amino acid zwitterion stability: Results from infrared action spectroscopy," J. Am. Chem. Soc. **130**, 6463–6471 (2008).

[5] M. F. Bush, J. Oomens, and E. R. Williams, "Proton affinity and zwitterion stability: New results from infrared spectroscopy and theory of cationized lysine and analogues in the gas phase," J. Phys. Chem. A **113**, 431–438 (2009).

[6] C. Kapota, J. Lemaire, P. Maître, and G. Ohanessian, "Vibrational signature of charge solvation vs salt bridge isomers of sodiated amino acids in the gas phase," J. Am. Chem. Soc. **126**, 1836–1842 (2004).

[7] R. C. Dunbar, A. C. Hopkinson, J. Oomens, C.-K. Siu, K. W. M. Siu, J. D. Steill, U. H. Verkerk, and J. Zhao, "Conformation switching in gas-phase complexes of histidine with alkaline earth ions," J. Phys. Chem. B **113**, 10403–10408 (2009).

[8] P. B. Armentrout, M. T. Rodgers, J. Oomens, and J. D. Steill, "Infrared multiphoton dissociation spectroscopy of cationized serine: Effects of alkali-metal cation size on gas-phase conformation," J. Phys. Chem. A **112**, 2248–2257 (2008).

[9] N. C. Polfer, J. Oomens, D. T. Moore, G. von Helden, G. Meijer, and R. C. Dunbar, "Infrared spectroscopy of phenylalanine Ag(I) and Zn(II) complexes in the gas phase," J. Am. Chem. Soc. **128**, 517–525 (2006).

[10] R. A. Coates, G. C. Boles, C. P. McNary, G. Berden, J. Oomens, and P. B. Armentrout, "Zn^{2+} and Cd^{2+} cationized serine complexes: Infrared multiple photon dissociation spectroscopy and density functional theory investigations," Phys. Chem. Chem. Phys. **18**, 22434–22445 (2016).

[11] G. C. Boles, R. L. Hightower, G. Berden, J. Oomens, and P. B. Armentrout, "Zinc and cadmium complexation of L-threonine: An infrared multiple photon dissociation spectroscopy and theoretical study," J. Phys. Chem. B **123**, 9343–9354 (2019).

[12] M. W. Forbes, M. F. Bush, N. C. Polfer, J. Oomens, R. C. Dunbar, E. R. Williams, and R. A. Jockusch, "Infrared spectroscopy of arginine cation complexes: Direct observation of gas-phase zwitterions," J. Phys. Chem. A **111**, 11759–11770 (2007).

[13] S. Firestein and G. M. Shepherd, "Interaction of anionic and cationic currents leads to a voltage dependence in the odor response of olfactory receptor neurons," J. Neurophysiol. **73**, 562–567 (1995).

[14] S. Frings, D. Reuter, and S. J. Kleene, "Neuronal Ca^{2+}-activated Cl^- channels—Homing in on an elusive channel species," Prog. Neurobiol. **60**, 247–289 (2000).

[15] M. Chesler, "Regulation and modulation of pH in the brain," Physiol. Rev. **83**, 1183–1221 (2003).

[16] G. Fenalti, P. M. Giguere, V. Katritch, X.-P. Huang, A. A. Thompson, V. Cherezov, B. L. Roth, and R. C. Stevens, "Molecular control of δ-opioid receptor signalling," Nature **506**, 191–196 (2014).

[17] S. J. Philips, M. Canalizo-Hernandez, I. Yildirim, G. C. Schatz, A. Mondragón, and T. V. O'Halloran, "Allosteric transcriptional regulation via changes in the overall topology of the core promoter," Science **349**, 877–881 (2015).

[18] N. Heine and K. R. Asmis, "Cryogenic ion trap vibrational spectroscopy of hydrogen-bonded clusters relevant to atmospheric chemistry," Int. Rev. Phys. Chem. **34**, 1–34 (2015).

[19] S. Tanabe, K. Hirata, K. Tsukiyama, J. M. Lisy, S.-i. Ishiuchi, and M. Fujii, "Can Ag^+ permeate through a potassium ion channel? A bottom-up approach by infrared spectroscopy of the Ag^+ complex with the partial peptide of a selectivity filter," J. Phys. Chem. Lett. **14**, 2886–2890 (2023).

[20] K. X. Vo, K. Hirata, J. M. Lisy, S.-i. Ishiuchi, and M. Fujii, "Na^+ selective binding by beauvericin and its mechanism studied by mass-coupled cold ion trap infrared spectroscopy," J. Phys. Chem. Lett. **13**, 11330–11334 (2022).

[21] J. T. O'Brien, J. S. Prell, G. Berden, J. Oomens, and E. R. Williams, "Effects of anions on the zwitterion stability of Glu, His and Arg investigated by IRMPD spectroscopy and theory," Int. J. Mass Spectrom. **297**, 116–123 (2010).

[22] J. Schmidt and S. R. Kass, "Zwitterion vs neutral structures of amino acids stabilized by a negatively charged site: Infrared photodissociation and computations of proline–chloride anion," J. Phys. Chem. A **117**, 4863–4869 (2013).

[23] M. Burt, K. Wilson, R. Marta, M. Hasan, W. Scott Hopkins, and T. McMahon, "Assessing the impact of anion–π effects on phenylalanine ion structures using IRMPD spectroscopy," Phys. Chem. Chem. Phys. **16**, 24223–24234 (2014).

[24] D. Corinti, B. Gregori, L. Guidoni, D. Scuderi, T. B. McMahon, B. Chiavarino, S. Fornarini, and M. E. Crestoni, "Complexation of halide ions to tyrosine: Role of non-covalent interactions evidenced by IRMPD spectroscopy," Phys. Chem. Chem. Phys. **20**, 4429–4441 (2018).

[25] E. M. Milner, M. G. D. Nix, and C. E. H. Dessent, "Collision-induced dissociation of halide ion–arginine complexes: Evidence for anion-induced zwitterion formation in gas-phase arginine," J. Phys. Chem. A **116**, 801–809 (2012).

[26] H. Zhang, W. Cao, Q. Yuan, X. Zhou, M. Valiev, S. R. Kass, and X.-B. Wang, "Cryogenic 'iodide-tagging' photoelectron spectroscopy: A sensitive probe for specific binding sites of amino acids," J. Phys. Chem. Lett. **11**, 4346–4352 (2020).

[27] W. Cao, H. Zhang, Q. Yuan, X. Zhou, S. R. Kass, and X.-B. Wang, "Observation of conformational simplification upon N-methylation on amino acid iodide clusters," J. Phys. Chem. Lett. **12**, 2780–2787 (2021).

[28] W. Cao, H. Zhang, Q. Yuan, X. Zhou, S. R. Kass, and X.-B. Wang, "Observation and exploitation of spin–orbit excited dipole-bound states in ion–molecule clusters," J. Phys. Chem. Lett. **12**, 11022–11028 (2021).

[29] Q. Yuan, W. Cao, and X.-B. Wang, "Cryogenic and temperature-dependent photoelectron spectroscopy of metal complexes," Int. Rev. Phys. Chem. **39**, 83–108 (2020).

[30] D. Hanstorp and M. Gustafsson, "Determination of the electron affinity of iodine," J. Phys. B: At., Mol. Opt. Phys. **25**, 1773 (1992).

[31] X.-B. Wang, Y.-L. Wang, J. Yang, X.-P. Xing, J. Li, and L.-S. Wang, "Evidence of significant covalent bonding in $Au(CN)_2^-$," J. Am. Chem. Soc. **131**, 16368–16370 (2009).

[32] T. Lu, Molclus program, version 1.9.9.9, http://www.keinsci.com/research/molclus.html (retrieved July 20, 2021).

[33] C. Bannwarth, S. Ehlert, and S. Grimme, "GFN2-xTB—An accurate and broadly parametrized self-consistent tight-binding quantum chemical method with multipole electrostatics and density-dependent dispersion contributions," J. Chem. Theory Comput. **15**, 1652–1671 (2019).

[34] Y. Zhao and D. G. Truhlar, "The M06 suite of density functionals for main group thermochemistry, thermochemical kinetics, noncovalent interactions, excited states, and transition elements: Two new functionals and systematic testing of four M06-class functionals and 12 other functionals," Theor. Chem. Acc. **120**, 215–241 (2008).

[35] F. Weigend and R. Ahlrichs, "Balanced basis sets of split valence, triple zeta valence and quadruple zeta valence quality for H to Rn: Design and assessment of accuracy," Phys. Chem. Chem. Phys. **7**, 3297–3305 (2005).

[36] S. Grimme, J. Antony, S. Ehrlich, and H. Krieg, "A consistent and accurate ab initio parametrization of density functional dispersion correction (DFT-D) for the 94 elements H-Pu," J. Chem. Phys. **132**, 154104 (2010).

[37] M. Walker, A. J. A. Harvey, A. Sen, and C. E. H. Dessent, "Performance of M06, M06-2X, and M06-HF density functionals for conformationally flexible anionic clusters: M06 functionals perform better than B3LYP for a model system with dispersion and ionic hydrogen-bonding interactions," J. Phys. Chem. A **117**, 12590–12600 (2013).

[38] G. D. Purvis III and R. J. Bartlett, "A full coupled-cluster singles and doubles model: The inclusion of disconnected triples," J. Chem. Phys. **76**, 1910–1918 (1982).

[39] K. Raghavachari, G. W. Trucks, J. A. Pople, and M. Head-Gordon, "A fifth-order perturbation comparison of electron correlation theories," Chem. Phys. Lett. **157**, 479–483 (1989).

[40] T. H. Dunning, Jr., "Gaussian basis sets for use in correlated molecular calculations. I. The atoms boron through neon and hydrogen," J. Chem. Phys. **90**, 1007–1023 (1989).

[41] R. A. Kendall, T. H. Dunning, Jr., and R. J. Harrison, "Electron affinities of the first-row atoms revisited. Systematic basis sets and wave functions," J. Chem. Phys. **96**, 6796–6806 (1992).

[42] K. A. Peterson, D. Figgen, E. Goll, H. Stoll, and M. Dolg, "Systematically convergent basis sets with relativistic pseudopotentials. II. Small-core pseudopotentials and correlation consistent basis sets for the post-d group 16–18 elements," J. Chem. Phys. **119**, 11113–11123 (2003).

[43] F. Neese, "The ORCA program system," Wiley Interdiscip. Rev.: Comput. Mol. Sci. **2**, 73–78 (2012).

[44] F. Neese, "Software update: The ORCA program system—Version 5.0," Wiley Interdiscip. Rev.: Comput. Mol. Sci. **12**, e1606 (2022).

[45] M. J. Frisch, G. W. Trucks, H. B. Schlegel, G. E. Scuseria, M. A. Robb, J. R. Cheeseman, G. Scalmani, V. Barone, G. A. Petersson, H. Nakatsuji, X. Li, M. Caricato, A. V. Marenich, J. Bloino, B. G. Janesko, R. Gomperts, B. Mennucci, H. P. Hratchian, J. V. Ortiz, A. F. Izmaylov, J. L. Sonnenberg, D. Williams-Young, F. Ding, F. Lipparini, F. Egidi, J. Goings, B. Peng, A. Petrone, T. Henderson, D. Ranasinghe, V. G. Zakrzewski, J. Gao, N. Rega, G. Zheng, W. Liang, M. Hada, M. Ehara, K. Toyota, R. Fukuda, J. Hasegawa, M. Ishida, T. Nakajima, Y. Honda, O. Kitao, H. Nakai, T. Vreven, K. Throssell, J. A. Montgomery, Jr., J. E. Peralta, F. Ogliaro, M. J. Bearpark, J. J. Heyd, E. N. Brothers, K. N. Kudin, V. N. Staroverov, T. A. Keith, R. Kobayashi, J. Normand, K. Raghavachari, A. P. Rendell, J. C. Burant, S. S. Iyengar, J. Tomasi, M. Cossi, J. M. Millam, M. Klene, C. Adamo, R. Cammi, J. W. Ochterski, R. L. Martin, K. Morokuma, O. Farkas, J. B. Foresman, and D. J. Fox, Gaussian 16, Gaussian, Inc., Wallingford, CT, 2016.

[46] V. A. Mozhayskiy and A. I. Krylov, ezSpectrum, http://iopenshell.usc.edu/downloads (retrieved December 10, 2015).

14 August 2023 10:42:37

[47] D. W. Arnold, S. E. Bradforth, E. H. Kim, and D. M. Neumark, "Study of $I^-(CO_2)_n$, $Br^-(CO_2)_n$, and $I^-(N_2O)_n$ clusters by anion photoelectron spectroscopy," J. Chem. Phys. **102**, 3510–3518 (1995).

[48] G.-L. Hou and X.-B. Wang, "Spectroscopic signature of proton location in proton bound $HSO_4^- \cdot H^+ \cdot X^-$ (X = F, Cl, Br, and I) clusters," J. Phys. Chem. Lett. **10**, 6714–6719 (2019).

[49] L. Wang, Q. Yuan, W. Cao, J. Han, X. Zhou, S. Liu, and X.-B. Wang, "Probing orientation-specific charge-dipole interactions between hexafluoroisopropanol and halides: A joint photoelectron spectroscopy and theoretical study," J. Phys. Chem. A **124**, 2036–2045 (2020).

[50] H. Zhang, W. Cao, Q. Yuan, L. Wang, X. Zhou, S. Liu, and X.-B. Wang, "Spectroscopic evidence for intact carbonic acid stabilized by halide anions in the gas phase," Phys. Chem. Chem. Phys. **22**, 19459–19467 (2020).

[51] L. J. Radziemski and V. Kaufman, "Wavelengths, energy levels, and analysis of neutral atomic chlorine (Cl I)," J. Opt. Soc. Am. **59**, 424–443 (1969).

[52] U. Berzinsh, M. Gustafsson, D. Hanstorp, A. Klinkmüller, U. Ljungblad, and A.-M. Mårtensson-Pendrill, "Isotope shift in the electron affinity of chlorine," Phys. Rev. A **51**, 231–238 (1995).

[53] C. Blondel, P. Cacciani, C. Delsart, and R. Trainham, "High-resolution determination of the electron affinity of fluorine and bromine using crossed ion and laser beams," Phys. Rev. A **40**, 3698–3701 (1989).

[54] Z. Tian and S. R. Kass, "Does electrospray ionization produce gas-phase or liquid-phase structures?," J. Am. Chem. Soc. **130**, 10842–10843 (2008).

[55] M. Bakhtiari and L. Konermann, "Protein ions generated by native electrospray ionization: Comparison of gas phase, solution, and crystal structures," J. Phys. Chem. B **123**, 1784–1796 (2019).

[56] Q. Yuan, W. Feng, W. Cao, Y. Zhou, L. Cheng, and X.-B. Wang, "Sodium cationization enables exotic deprotonation sites on gaseous mononucleotides," J. Phys. Chem. Lett. **13**, 9975–9982 (2022).

14 August 2023 10:42:37